

RESEARCH

Open Access



Artificial Hummingbird Algorithm-based fault location optimization for transmission line

Sushma Verma^{1*}, Provas Kumar Roy², Barun Mandal² and Indranil Mukherjee³

*Correspondence:
sushma.verma1976@gmail.com

¹ Techno International New
Town, Kolkata, India

² Kalyani Government
Engineering College, Kalyani,
India

³ AliahUniversity, Kolkata, India

Abstract

Transmission is an important aspect regarding an effective designing of electric supply system. Ensuring reliable and fault-free transmission from the source for effective distribution to the end consumers is very much desirable. In this respect, fast and accurate fault detection, particularly in the overhead transmission lines, is very pertinent. Various algorithms and novel approaches have been formulated by various researchers aligned to this challenge. In this context, a new algorithm influenced by the biotic procedure of flight skills of hummingbird seems to be one of the best algorithms to address the cited problem. This paper focuses on the formulation of this Artificial Hummingbird Algorithm (AHA) and its high accuracy in ameliorating the fault location in transmission line. The most common flight skills being used in the algorithm are foraging schemes, which includes axial, diagonal, and omnidirectional flights. The proposed AHA has been tested using the Simulink prototype in MATLAB for an overhead transmission line having a length of 300 km and system voltage of 400 kV at suitable lengths. Specimen signal of voltages and currents waveforms has been taken at duo ends of the overhead transmission line. The results of the proposed algorithm have been compared with the results obtained from previous studies, and it has been observed that this algorithm yields better results for various kinds of asymmetrical and symmetrical faults.

Keywords: Artificial Hummingbird Algorithm, Current signal, Fault location, Fitness function, Simulink, Transmission line and voltage signal

Introduction

One of the most important factors for efficient designing of an electric power system is the precise and fast detection of faults in the transmission line. Researchers and academicians along with industry persons, all across the globe, have carried out various studies regarding different methods for an effective designing of a power system. The main objective of their studies is centered around the most rapid and precise detection of faults in the transmission lines. Regarding locating the location of faults, [1–10] have all conducted studies to confirm the effective location of faults.

In general, fault locating algorithms which are applied are broadly categorized into two groups. In the first group, potential and ampere signals are evaluated only at single end [1–3]. In the second group, potential and ampere signals have been evaluated at duo

ends of the line [4, 11]. The findings of the studies have indeed put forth the need for a better algorithm to be framed for addressing the problem. In this regard, a novel optimization algorithm stimulated by biological instinct of hummingbirds, known as AHA, has been elaborately discussed in the current study. Researchers, namely Zhao [12] and Ramadan [13], have effectively applied the AHA for engineering design case studies and accurate models for solar cell systems, respectively, and their findings have reported that AHA yields excellent results compared to the other methods used. The hazards associated with the overhead lines are magnified by their ubiquitous exposure to the atmosphere and to different natural disturbances and inherited short circuit faults. The proposed AHA in the study functions as the fault locator and works to readily identify the fault point and thereby to improve the reliability and performance of the power system. This is even more so important to justify a sturdy transient detecting system [14]. Generally, applied techniques for fault location can be categorized mainly as follows:

- i) Methods grounded on impedance measurement [15–17]
- ii) Methods based on travelling waves [3, 18–22]
- iii) Methods dependent on the higher frequency constituents of potentials and amperes caused by symmetrical and unsymmetrical faults on transmission line, known as faults-based methods [23, 24].
- iv) Intelligent retrieval grounded techniques like artificial neural networks (ANN), machine learning [25], support vector regression [26], genetic algorithm (GA) [27], and deep learning [28–32]
- v) The fuzzy logic systems [33, 34]
- vi) Methods based on the wavelet analysis techniques [35, 36]

All the methods mentioned above suffer from some kind of drawbacks based on particular constraints as far as fault locating is concerned. The proposed AHA is based on three flying and foraging skills of hummingbirds, which encompasses all the technical attributes required regarding the effective location of faults and thereby to address them subsequently.

The study reports on the findings using the stated AHA with previous studies conducted using the other fault location techniques mentioned above and justify the higher acceptability and accuracy of AHA in comparison to them.

Throughout the past several decades, various optimization techniques have been developed for solving the loads of optimization challenges in various fields of day-to-day life [37, 38]. In contemporary years, nevertheless, the complexity of actual optimization issues has turned up considerably with the growth of human community and present industry operations. Principally, the current optimization methodologies can be characterized into deterministic and metaheuristic algorithm (routines).

Deterministic routines are particular arithmetical algorithms and functions cyclically and repetitively devoid of any unpredictable characteristics. On a stated problem, a deterministic approach invariably acquires the identical result for a specific information.

The metaheuristic algorithm has merits which enable this algorithm to efficiently search universal optimal answers to given challenges that deterministic methods cannot answer. Bioinspired algorithms have attained the maximum acceleration among these

methods and are progressively implemented on different engineering problems successfully [39–42]

Methods

Aim of the study

The main aim of the study is to find the accurate location of the fault point.

Design of the study

For solving the challenge of accurate fault location, first of all, Simulink model of the transmission line is constructed in MATLAB as shown in Fig. 3A and explained in “[Simulink model](#)” section. To optimize the fault location point, a fitness function is formulated on the basis of travelling wave theory. The difference of the voltage at the fault point as seen from sending end and receiving end should be zero. Considering this fact, fitness function is formulated on the basis of the equations for the voltage at the sending end and receiving end as explained in the “[Formulation of fitness function](#)” section. These equations are constructed on the principle of travelling wave theory as explained in the “[Formulation of fitness function](#)” section. The voltage at the sending end and receiving end is illustrated in Eqs. (10) and (11). AHA is used to optimize the fault location point. The algorithm is run in MATLAB.

Methodology used

The methodology used including the introduction to the algorithm used is explained in subsequent “[Artificial Hummingbird Algorithm \(AHA\)](#)” and “[Results and discussion](#)” sections. All the required signals are taken from the Simulink model after running the required programs in MATLAB.

Artificial Hummingbird Algorithm (AHA)

Introduction to the algorithm

This algorithm is inspired by biological process, rooted on intellectual conducts of hummingbirds. The hummingbirds by virtue of their ease in mobility are capable of moving from one location to the other at a ready pace; also, the locations once visited (called the hunt areas) are retained in their memories. They efficiently remember the information about individual florets for a particular area counting the location of flower, quality of the nectar, and the time they travelled to the flower. Keeping all these information, hummingbirds decide where to visit next for their nourishment and refrain from returning to recently visited flowers. Three main foraging models of hummingbirds, which includes guided foraging, territorial foraging, and migration foraging, are explained as follows [12].

Guided foraging

The arithmetical equation imitating the guided foraging is formulated as follows:

$$v1_i(t + 1) = x1_{i,tar}(t) + a1.D1.(x1_i(t) - x1_{i,tar}(t)) \quad (1)$$

$$a1 \sim N(0, 1) \tag{2}$$

where $x1_i(t)$ denotes the position of i^{th} meal origin at time t and $x1_{i,tar}(t)$ is the point of the desired meal source that the i^{th} hummingbird aspires to travel and where $a1$ is a directed component.

Territorial foraging

The following equation illustrates the local hunt of hummingbirds in the territorial foraging strategy:

$$v1_i(t + 1) = x1_i(t) + b1.D.x1_i(t) \tag{3}$$

$$b1 \sim N(0, 1) \tag{4}$$

where $b1$ is a factor related with territory.

Migration foraging

The arithmetical equation for the migration foraging of a hummingbird is denoted as follows:

$$x_{wor}(t + 1) = Low + r.(Up - Low) \tag{5}$$

where x_{wor} is the food origin with the poorest rate of nectar replenishment, r is a random factor, and up and low are the upper and lower limit ranges, respectively.

The fitness function forms the basis of the algorithm which is explained in the following section.

Formulation of fitness function

The proposed AHA is based primarily on the formulation of fitness function which serves as the platform for optimization to arrive precisely and readily at the fault location in the transmission line. Figure 1 represents the single-phase prototype of a three-phase transmission line assuming distributed parameters [43, 44]. A_s and A_R represent the voltage sources at sending terminal and the receiving terminal respectively of phase A in Fig. 1 [45].

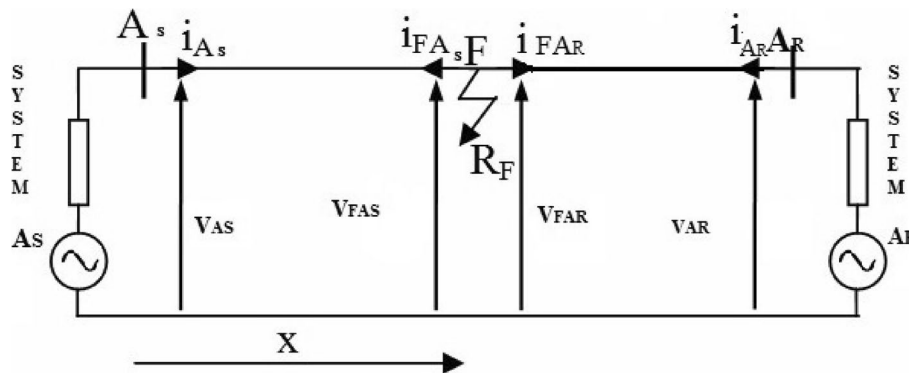


Fig. 1 Single-phase prototype of three-phase line

The distributed model of transmission line from sending end (S) to fault point (F) segment of the transmission wire is reflected in Fig. 2.

The following equations are obtained in accordance with Fig. 2 [46].

$$i_s(t) = \frac{1}{Z_c} * V_s(t) + I_r(t - \tau) \tag{6}$$

$$i_x(t) = \frac{1}{Z_c} * V_x(t) + I_x(t - \tau) \tag{7}$$

I_r and I_x in Eqs. (6) and (7) represent dependant current sources respectively and are defined as follows:

$$i_r(t - \tau) = \frac{-R'}{Z_c'^2} [V_s(t - \tau) + Z_c'' * i_s(t - \tau)] - \frac{Z_c}{Z_c'^2} [V_x(t - \tau) + Z_c'' * i_x(t - \tau)] \tag{8}$$

$$i_x(t - \tau) = \frac{-R'}{Z_c'^2} [V_x(t - \tau) + Z_c'' * i_x(t - \tau)] - \frac{Z_c}{Z_c'^2} [V_s(t - \tau) + Z_c'' * i_s(t - \tau)] \tag{9}$$

where

τ = Time elapsed for the wave to propagate from sending terminal to fault terminal.

Z_c = Characteristic impedance of transmission wire.

R' = Resistance of line from sending end(S) to fault point (F)

$$Z_c' = Z_c + \frac{R'}{4}$$

$$Z_c'' = Z_c - \frac{R'}{4}$$

Cancelling the current i_x from Eqs. (6, 7, 8 and 9) the voltage at the point of fault location can be formulated as function of sending end voltage and current as in Eq. (10).

$$V_{xs}(t) = \frac{\left(Z_c'^2 [V_s(t + \tau) - Z_c' * i_s(t + \tau)] + Z_c''^2 [V_s(t - \tau) + Z_c'' * i_s(t - \tau)] - \left(\frac{Z_c R'}{4} \right) * \left[\frac{R'}{Z_c} * V_s(t) + 2 * Z_c'' * i_s(t) \right] \right)}{2 * Z_c^2} \tag{10}$$

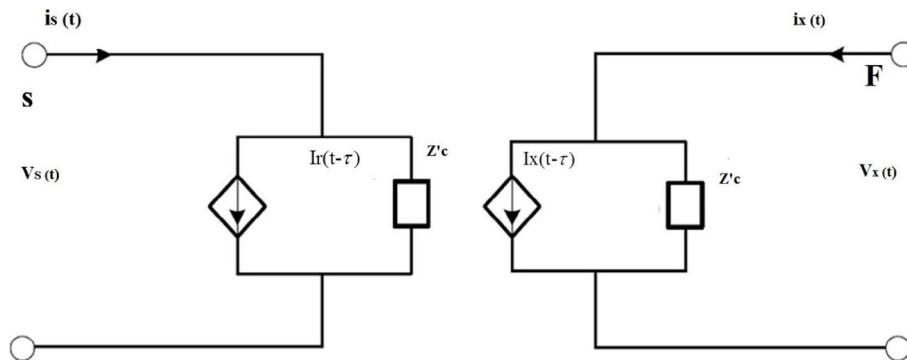


Fig. 2 Distributed prototype of overhead transmitting wire (S to F segment)

Similarly, the voltage at the point of fault location can be formulated as function of receiving end voltage and current as in Eq. (11).

$$V_{xr}(t) = \frac{\left(Z_c'^2 [V_R(t + T - \tau) - Z_{rc}' * i_R(t + T - \tau)] + Z_c''^2 [V_R(t - T + \tau) + Z_{rc}'' * i_R(t - T + \tau)] - \frac{Z_{rc}' * R_r'}{4} * \left[\frac{R_r'}{Z_{rc}'} * V_R(t) + 2 * Z_{rc}'' * i_R(t) \right] \right)}{2 * Z_c^2} \tag{11}$$

where:

T = Time taken for the wave to propagate from sending terminal (S) to receiving terminal (R)

R_r = Line resistance from receiving end (R) to fault point (F)

$$Z_{rc}' = Z_c + \frac{R_r'}{4}$$

$$Z_{rc}'' = Z_c - \frac{R_r'}{4}$$

The voltage at the point of occurrence of fault should be lone in any instance of the data utilized for the calculation [47]. In view of this, the two extracted voltages must be equivalent at all times. As the potential through the overhead wire is continual, Eqs. (10) and (11) can be merged leading to the following equation

$$F(V_s, i_s, V_r, i_r, t, \tau) = V_{xs}(t) - V_{xr}(t) \tag{12}$$

Equation (12) ought to be correct as the variation between the voltages must be zero. Where the function F is defined as follows:

$$F = \left(Z_c'^2 [V_s(t + \tau) - Z_c' * i_s(t + \tau)] + Z_c''^2 [V_s(t - \tau) + Z_c'' * i_s(t - \tau)] - \frac{Z_c' * R_r'}{4} \left[\frac{R_r'}{Z_c'} * V_s(t) + 2 * Z_c'' * i_s(t) \right] - \left(Z_{rc}' [V_R(t + T - \tau) - Z_{rc}' * i_R(t + T - \tau)] + Z_{rc}''^2 [V_R(t - T + \tau) + Z_{rc}'' * i_R(t - T + \tau)] - \frac{Z_{rc}' * R_r'}{4} \left[\frac{R_r'}{Z_{rc}'} * V_R(t) + 2 * Z_{rc}'' * i_R(t) \right] \right) \right) / 2 * Z_c^2 \tag{13}$$

Equation (13) is the fitness function which has to be minimized to assess the point of fault. In this paper, the fitness function is minimized utilizing AHA.

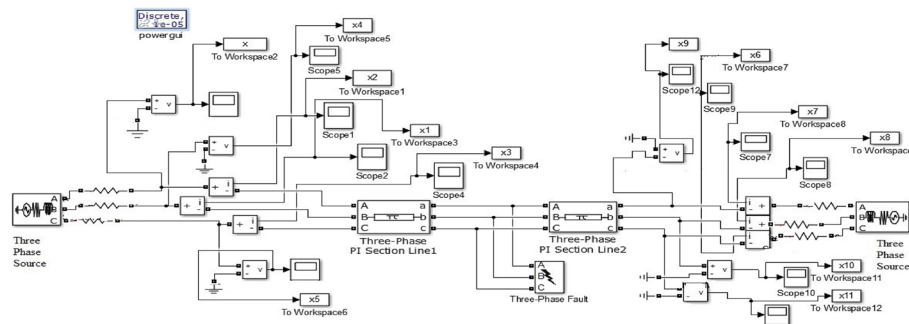


Fig. 3 Simulink model of the system under study

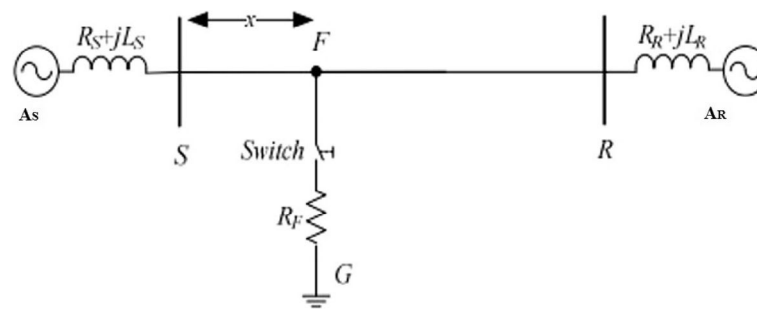


Fig. 4 System under study

Table 1 Parameters of transmission line

Parameter	Value
R (positive)	0.0275 Ω /km
R (zero)	0.275 Ω /km
L (positive)	1.002768 mH/km
L (zero)	3.4505998 mH/km
C (positive)	13 nF/km
C (zero)	8.5 nF/km

Simulink model

The Simulink model of the system as shown in Fig. 3 below is simulated in MATLAB. The sending end and receiving end voltage and current signals from this model are used in fitness function which is formulated in Eq. 13 and subsequently for running of AHA.

Results and discussion

Suggested method

In this proposed study, AHA is run in MATLAB to get the fault point on the basis of formulated objective function. The Simulink of the network being investigated is illustrated in Fig. 3. The single-line diagram of the system is shown in Fig. 4 below.

The parameters of transmission line are denoted in Table 1 [48]. The nominal voltage of power system is 400 kV with system frequency as 50 HZ. Phase angle difference between sending end and receiving end voltage sources is 25° . The error % is calculated as per the formula given in Eq. (14).

$$E_{FL} = [(X_{CALCULATED} - X_{REAL}) / L] \times 100 \quad (14)$$

where:

$X_{CALCULATED}$ is the calculated location

X_{REAL} is real location

L is total length of line

Various cases of faults at different spans have been simulated, which have been reported in the subsequent sections.

Table 2 Simulation results for fault occurring at 10 km from sending end

Fault type	Calculated location of fault error	%age absolute
A-G	9.9856	0.004
B-G	10.0205	0.006
C-G	10	0
AB-G	10.0205	0.006
BC-G	9.9973	0.0009
CA-G	10.0126	0.004
ABC-G	10.0531	0.01

Table 3 Simulation results for fault for fault occurring at 50 km from sending end

Fault type	Calculated location of fault error	%age absolute
A-G	49.9856	0.005
B-G	49.9272	0.02
C-G	49.9763	0.008
AB-G	50.012	0.004
BC-G	49.9682	0.01
CA-G	49.9574	0.01
ABC-G	49.6434	0.01

Table 4 Simulation results for fault occurring at 100 km from sending end

Fault type	Calculated location of fault error	%age absolute
A-G	100.01	0.003
B-G	100.0236	0.008
C-G	99.9982	0.0006
AB-G	100.0213	0.007
BC-G	99.9962	0.001
CA-G	100.113	0.0004
ABC-G	99.9987	0.0037

Table 5 Simulation results for fault occurring at 200 km from sending end

Fault type	Calculated location of fault error	%age absolute
A-G	199.985	0.005
B-G	200.0123	0.004
C-G	200.101	0.03
AB-G	200	0
BC-G	199.9763	0.007
CA-G	200.0112	0.004
ABC-G	199.9815	0.006

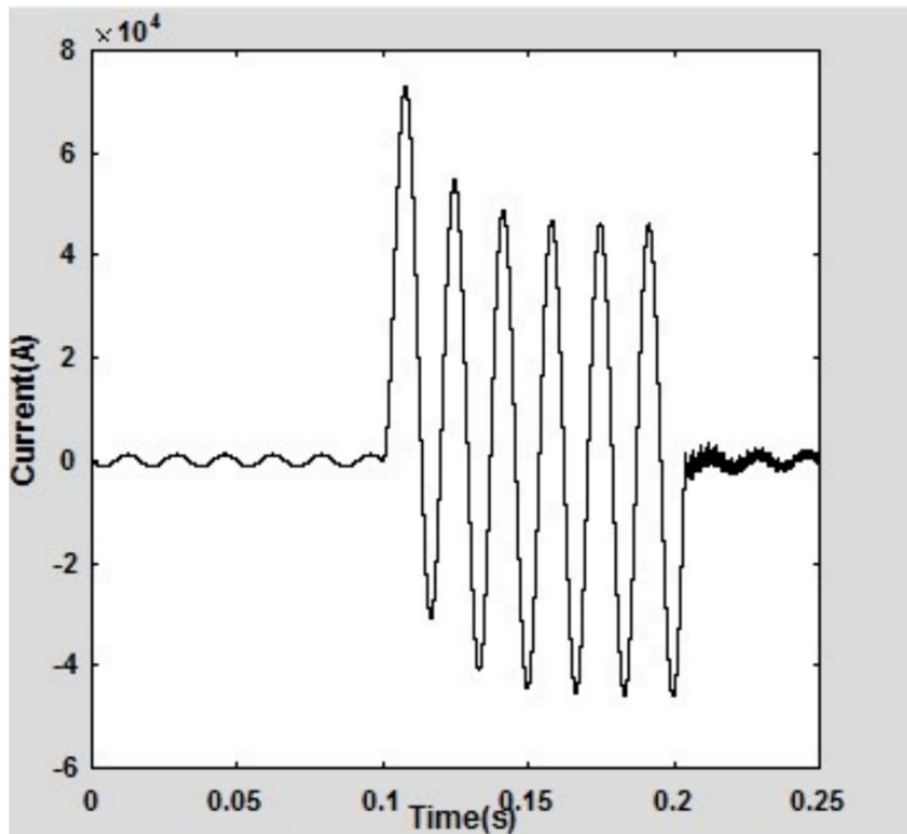


Fig. 5 Simulated current signal recorded at a distance of 10 km against the sending point for A-G fault, bearing fault resistance value as 0.00001 Ω

Table 6 Simulation results for transient existing a stretch of 10 km against sending station bearing resistance of fault path as 10 Ω

Fault type	Calculated location of fault error	%age absolute
A-G	9.9804	0.006
B-G	10.0119	0.004
C-G	9.9973	0.0009
AB-G	10.0217	0.007
BC-G	10.0014	0.0005
CA-G	9.9978	0.0007
ABC-G	10.0264	0.009

Impact of fault type and location

Various kinds of faults simulated are phase A to ground (A-G), phase B to ground (B-G), phase C to ground (C-G), phase A to phase B to ground (AB-G), phase B to phase C to ground (BC-G), phase C to phase A to ground (CA-G), and phase A to phase B to phase C to ground (ABC-G) with value of fault resistance as 0.00001 Ω. Results for localization of fault in transmission line are presented in Tables 2, 3, 4, and 5.

Table 7 Simulation results for transient existing at a stretch of 10 km against sending station bearing resistance of fault path as 50 Ω

Fault type	Calculated location of fault error	%age absolute
A-G	9.9864	0.005
B-G	10.0126	0.004
C-G	10.1073	0.0036
AB-G	9.9768	0.008
BC-G	9.9961	0.004
CA-G	9.8657	0.04
ABC-G	10.0254	0.008

Table 8 Simulation results for transient existing at a stretch of 10 km against sending station bearing resistance of fault path as 100 Ω

Fault type	Calculated location of fault error	%age absolute
A-G	9.9953	0.001
B-G	10.0197	0.006
C-G	10	0
AB-G	10.002	0.0007
BC-G	10.0174	0.006
CA-G	9.9876	0.004
ABC-G	10.0521	0.017

Table 9 Simulation results for transient existing against at a stretch of 50-km sending station bearing resistance of fault path as 10 Ω

Fault type	Calculated location of fault error	%age absolute
A-G	49.9763	0.008
B-G	49.935	0.02
C-G	50.0123	0.004
AB-G	50.0658	0.02
BC-G	49.9871	0.004
CA-G	50.0234	0.008
ABC-G	50.0123	0.004

Table 10 Simulation results for transient existing at a stretch of 50 km against sending station bearing resistance of fault path as 50 Ω

Fault type	Calculated location of fault error	%age absolute
A-G	49.9531	0.02
B-G	50.0476	0.02
C-G	49.9154	0.03
AB-G	49.7829	0.07
BC-G	49.9967	0.001
CA-G	50.0679	0.02
ABC-G	50.0012	0.0004

Table 11 Simulation results for transient existing at a stretch of 50 km against sending station bearing resistance of fault path as 100 Ω

Fault type	Calculated location of fault error	%age absolute
A-G	49.9962	0.001
B-G	50.0035	0.001
C-G	50.0465	0.01
AB-G	50.123	0.04
BC-G	49.9967	0.001
CA-G	50.0798	0.02
ABC-G	49.9872	0.004

Table 12 Simulation results for transient existing at a stretch of 100 km against sending station bearing resistance of fault path as 10 Ω

Fault type	Calculated location of fault error	%age absolute
A-G	100.001	0
B-G	100.0175	0.006
C-G	99.9765	0.008
AB-G	100.0157	0.005
BC-G	99.892	0.04
CA-G	100.126	0.04
ABC-G	99.9965	0.001

Table 13 Simulation results for transient existing at a stretch of 100 km against sending station bearing resistance of fault path as 50 Ω

Fault type	Calculated location of fault error	%age absolute
A-G	99.9967	0.001
B-G	100.026	0.008
C-G	99.9873	0.004
AB-G	100.107	0.03
BC-G	99.9867	0.004
CA-G	100.002	0.0006
ABC-G	99.9793	0.007

Table 14 Simulation results for transient existing at a stretch of 100 km against sending station bearing resistance of fault path as 100 Ω

Fault type	Calculated location of fault error	%age absolute
A-G	100.1123	0.037
B-G	100.0347	0.011
C-G	99.8963	0.034
AB-G	99.9872	0.004
BC-G	100.0175	0.006
CA-G	100.012	0.004
ABC-G	99.8672	0.045

Table 15 Simulation results for transient existing at a stretch of 200 km against sending station bearing resistance of fault path as 10 Ω

Fault type	Calculated location of fault error	%age absolute
A-G	199.996	0.0013
B-G	200.0175	0.006
C-G	200	0
AB-G	200.123	0.04
BC-G	199.979	0.007
CA-G	200.114	0.038
ABC-G	199.8765	0.04

Table 16 Simulation results for transient existing at a stretch of 200 km against sending station bearing resistance of fault path as 50 Ω

Fault type	Calculated location of fault error	%age absolute
A-G	199.987	0.004
B-G	199.995	0.0017
C-G	199.865	0.045
AB-G	200.104	0.035
BC-G	200.012	0.004
CA-G	200.102	0.034
ABC-G	199.966	0.011

Table 17 Simulation results for transient existing at a stretch of 200 km against sending station bearing resistance of fault path as 100 Ω

Fault type	Calculated location of fault error	%age absolute
A-G	200.112	0.004
B-G	200.023	0.007
C-G	199.984	0.005
AB-G	199.987	0.004
BC-G	200.017	0.005
CA-G	199.97	0.01
ABC-G	200.126	0.042

Figure 5 shows the current waveform for A-G fault, occurring at a distance of 10 km from the sending end, having fault resistance value of 0.00001 Ω .

Impact of resistance of fault

Resistance of fault is a very important parameter which influences the correctness of methods for fault location. Hence, to estimate the influence of resistance of fault, simulations have been performed for numerous fault resistances (10, 50, and 100 Ω) with several fault types. Tables 6, 7, 8, 9, 10, 11, 12, 13, 14, 15, 16, and 17 show the respective results. Figure 6 shows the current waveform for B-G fault, occurring at a distance of 50 km from the sending point having fault resistance value as 10 Ω .

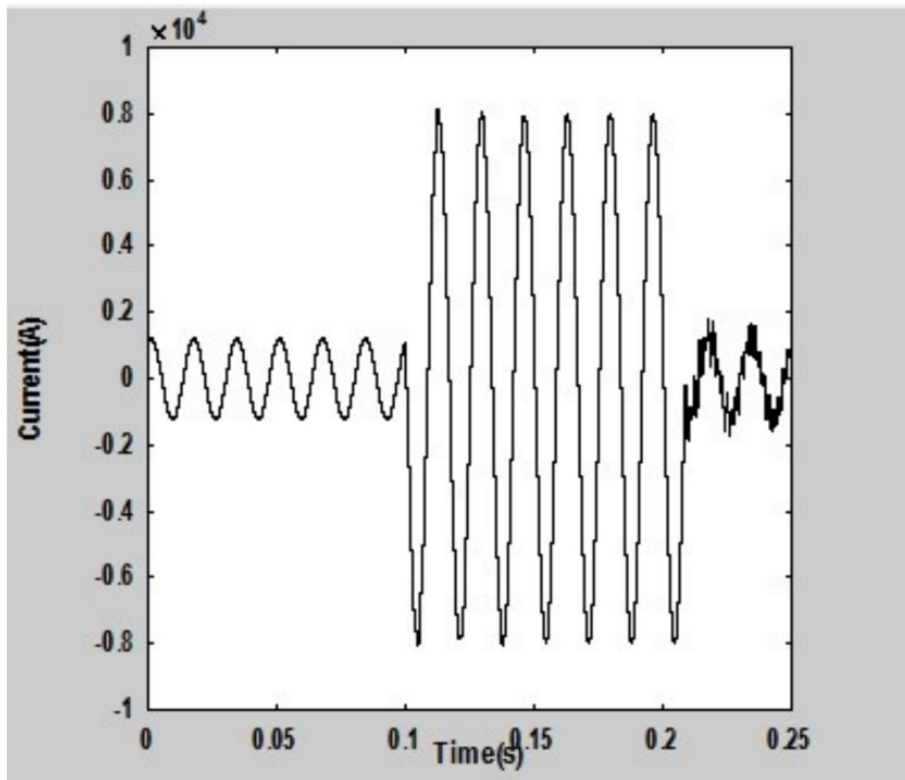


Fig. 6 Simulated current signal recorded at a distance of 50 km from sending point side for B-G fault bearing fault resistance value as $10\ \Omega$

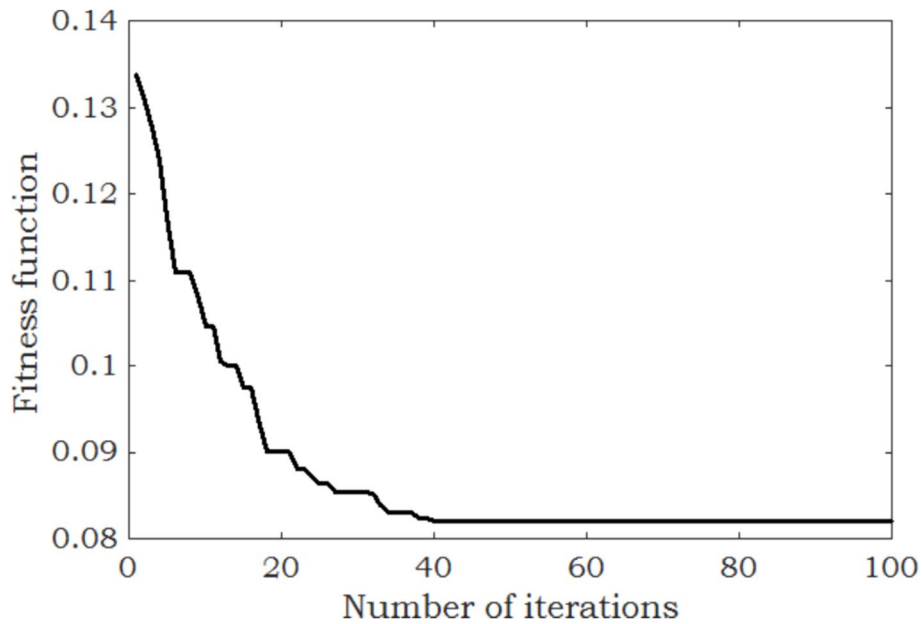


Fig. 7 Fitness graph for AB-G at a stretch of 10 km from sending terminal bearing resistance of fault path as $10\ \Omega$

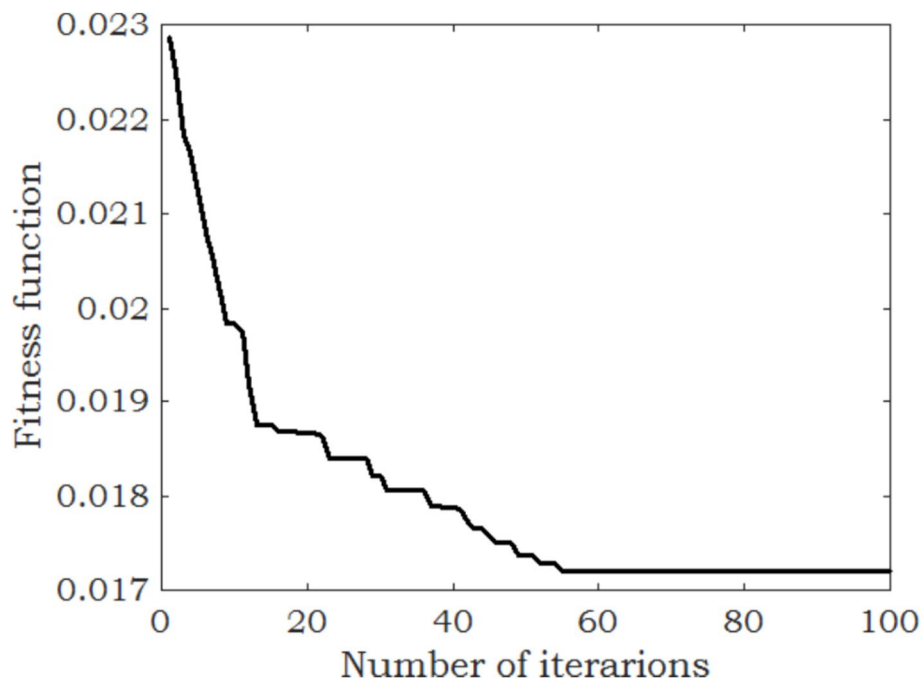


Fig. 8 Fitness graph for ABC-G at a stretch of 200 km from sending terminal bearing resistance of fault path as 50Ω

Fitness graphs for AB-G fault occurring at a distance of 10 km from sending point side with fault resistance of 10Ω and for ABC-G fault, occurring at 200-km distance from the sending point, and bearing fault resistance value of 50Ω are shown in Figs. 7 and 8, respectively.

Comparison with other studies

Takagi et al. [2] conducted the fault localization study and found that maximum and minimum error is 2.6% and 0.6%, respectively. Girgis et al. [4] reported that when electromagnetic transient program (EMTP) is used for locating the fault point, the maximum value of the error is less than 1%. The maximal fault location errors observed in the study conducted by Mustari et al. [49] and Lavand et al. [50] are 1.5% and 1%, respectively. A. Sanad Ahmed et al. [47] concluded that by using GA method with the value of fault resistance being 10Ω , the maximum value of percentage error is 0.13% and with fault resistance value of 50Ω is 0.068%. A. Sanad Ahmed et al. [47] concluded that by using Harmonic Search method (HS) with fault resistance value of 10Ω , the maximum value of percentage error is 0.178% and with fault resistance of 50Ω is 0.39%. A. Sanad Ahmed et al. [47] also concluded that by using method of teaching-learning-based optimization (TLBO) with fault resistance of 10Ω , the maximum value of percentage error is 0.13% and with fault resistance of 50Ω is 0.833%. Contrarily in the presented study, as established from Tables 2, 3, 4, and 5 with fault resistance value 0.00001Ω , the maximum magnitude of the absolute of the % age error in fault location is 0.03%, and with varying fault resistances, the study reveals from Tables 6, 7, 8, 9, 10, 11, 12, 13, 14, 15, 16, and 17, the maximum magnitude of the absolute of % age error in fault location is 0.04%. Consequently, higher precision

is acquired for the exhibited algorithm compared to the earlier revealed studies. It is also concluded that preciseness of location is hardly affected by kind of transient (fault) and fault resistance.

Conclusions

Precise and fast detection of fault locations form an intrinsic part of an effective transmission line design, and it is directly related to the efficiency associated with it. Previous studies conducted show that the percentage error obtained is higher in magnitude for the methods adopted in them compared to the method suggested in this paper. Hence, the method suggested in the study offers highly accurate diagnosis of fault locations in the transmission line.

Abbreviations

AHA	Artificial Hummingbird Algorithm
ANN	Artificial neural networks
A-G	Phase A to ground
B-G	Phase B to ground
C-G	Phase C to ground
AB-G	Phase A to phase B to ground
BC-G	Phase B to phase C to ground
ACG	Phase A to phase C to ground
ABC-G	Phase A to phase B to phase C to ground
GA	Genetic algorithm
HS	Harmonic search
TLBO	Teaching-learning-based optimization
EMTP	Electromagnetic transient program

Acknowledgements

The author acknowledges the effort of Prof. Bikash Patel of Kalyani Government Engineering College, Department of Electrical Engineering, for his valuable guidance in this study.

Authors' contributions

SV conducted the literature review. Based on the review and the previous study formulated, the transmission line model in Simulink calculated the required parameters and formulated the required equations. PR formulated and designed the required MATLAB program based on AHA and proposed Simulink model of transmission line and the formulated equations. He is a vital contributor in writing the manuscript. BM executed the various simulations for the offered Simulink model at diverse locations with varied fault cases for different values of fault resistances. IM analyzed and interpreted the results of fault localization with the previous study. All authors have thoroughly read and approved the manuscript.

Funding

Not applicable.

Availability of data and materials

The data whatever support the recommendations of this calculation are accessible against the concerning author over justifiable demand.

Declarations

Competing interests

The authors declare that they have no competing interests.

Received: 21 March 2023 Accepted: 19 June 2024

Published online: 08 July 2024

References

1. Eriksson L, Saha MM, Rockefeller G (1985) An accurate fault locator with compensation for apparent reactance in the fault resistance resulting from remote end infeed. *IEEE Trans Power App Syst* 5(2):44–44
2. Takagi T, Yamakoshi Y, Yamaura M, Kondow R, Matsushima T (1982) Development of a new type fault locator using the one-terminal voltage and current data. *IEEE Trans Power App Syst PAS-101* (8):2892–2898
3. Ibe A, Cory B (1986) A travelling wave-based fault locator for two-and three- terminal networks. *IEEE Transact Power Del* 1(2):283–288

4. Girgis AA, Hart DG, Peterson WL (1992) A new fault location technique for two- and three-terminal lines. *IEEE Transact Power Del* 7(1):98–107
5. Lu D, Liu Y, Lu D, Wang B, Zheng X (2022) Unsynchronized fault location on untransposed transmission lines with fully distributed parameter model considering line parameter uncertainties. *Electric Power Syst Res* 202:107622
6. Rezaei D, Gholipour M, Parvaresh F (2022) A single-ended traveling-wave-based fault location for a hybrid transmission line using detected arrival times and TWs. *Electric Power Syst Res* 210:108058
7. Xie J, Jin G, Wang Y, Ni X, Liu X (2022) New algorithm for 2-terminal transmission line fault location integrating voltage phasor feature and phase angle jump checking. *Electric Power Syst Res* 209:107971
8. Liang Y, Ding J, Li H, Wang G, Zhang Z (2022) Transmission line frequency-domain fault location method based on the phasor-time space curve characteristics that considers decaying DC deviation. *Int J Electric Power Energy Syst* 142:108308
9. Gaur VK, Bhalja BR, Saber, A. (2022) New ground fault location method for three-terminal transmission line using unsynchronized current measurements. *Int J Electric Power Energy Syst* 135:107513
10. Moradzadeh A, Teimourzadeh H, Mohammadi-Ivatloo B, Pourhossein K (2022) Hybrid CNN-LSTM approaches for identification of type and locations of transmission line faults. *Int J Electric Power Energy Syst* 135:107563
11. Johns A, Jamali S (1990) Accurate fault location technique for power transmission lines. *IEE Proceedings C (Generation, Transmission and Distribution)* 137(6):395–402
12. Zhao W, Wang L, Mirjalili S (2022) Artificial hummingbird algorithm: a new bio-inspired optimizer with its engineering applications. *Comput Methods Appl Mech Eng* 388:114194
13. Ramadan A, Kamel S, Hassan MH, Ahmed E.M. Hasanien, HM. (2022) Accurate photovoltaic models based on an adaptive opposition artificial hummingbird algorithm. *Electronics* 11(3):318
14. Mallaki M, Dashti R (2012) Fault locating in transmission networks using transient voltage data fault locating in transmission networks using transient voltage data. *Energy Procedia* 14:173–180
15. Dalcastagne A, Zimath S (2008) A study about the sources of error of impedance-based fault location methods a study about the sources of error of impedance-based fault location methods. *IEEE/PES Transmission and Distribution Conference and Exposition: Latin America. IEEE/pes*, pp 1–6. <https://doi.org/10.1109/TDC-LA.2008.4641697>.
16. Hashim MN, Osman MK, Ibrahim MN, Abidin AF (2017) Investigation of features extraction condition for impedance-based fault location in transmission lines. 7th IEEE International Conference on Control System, Computing and Engineering (ICCSCE). pp 325–330
17. Dzienis C, Yelgin Y, Washer M, Maun JC (2015) Accurate impedance based fault location algorithm using communication between protective relays. *Modern Electric Power Systems (MEPS)* 2015. pp 1–6
18. Naidu OP, AK. (2018) A traveling wave-based fault location method using unsynchronized current measurements. *IEEE Trans Power Delivery* 34(2):505–513
19. Mousaviyan I, Seifossadat SG, Saniei M (2022) Traveling wave based algorithm for fault detection, classification, and location in STATCOM compensated parallel transmission lines. *Electric Power Syst Res* 210:108118
20. Anane POK, Huang Q, Bamisile O, Ayimbire PN (2021) Fault location in overhead transmission line: a novel non-contact measurement approach for traveling wave based scheme. *Int J Electric Power Energy Syst* 133:107233
21. Abeid AM, Abd el Ghany HA, Azmy AM (2017) An advanced travelling wave fault location algorithm for simultaneous faults. Nineteenth International Middle East Power Systems Conference (MEPCON). pp 747–752
22. Lei A, Dong X, Shi S, Wang B (2015) A novel current travelling wave based single-ended fault location method for locating single-phase-to-ground fault of transmission line. 50th International Universities Power Engineering Conference (UPEC)
23. Huynh DC, Truong TH, Truong AV, Dunnigan MW (2019) Development of fault location for distributed parameter transmission lines of a power system. 2019 2nd International Conference on High Voltage Engineering and Power Systems (ICHVEPS)
24. Mardiana R, Al Motairy HSu, CQ. (2010) Ground fault location on a transmission line using high frequency transient voltages. *IEEE Transact Power Del* 26(2):1298–1299
25. Voutsinas S, Karolidis D, Voyiatzis I, Samarakou M (2023) Development of a machine-learning-based method for early fault detection in photovoltaic systems. *J Eng Appl Sci* 70:27
26. Amroune M (2022) Support vector regression bald eagle search optimizer based hybrid approach for short term wind power forecasting. *J Eng Appl Sci* 69:107
27. Geneid A, Atia M, Badawy (2022) A Multi-objective optimization of vertical axis wind turbine's blade structure using genetic algorithm. *J Eng Appl Sci* 69:90
28. Chaitanya B, Yadav A, Andanapalli K, Varma BR (2016) A comparative study of different signal processing techniques for fault location on transmission lines using hybrid generalized regression neural network. *International Conference on Signal Processing, Communication, Power and Embedded System (SCOPE)* 2016. pp 1246–1250
29. Jain A, Moses B (2016) Soft computing based fault detection & classification for transmission lines. *International Conference on Electrical, Electronics, and Optimization Techniques (ICEEOT)* 2016. pp 4061–4064
30. Saravanan N, Rathinam A (2012) A comparative study on ANN based fault location and classification technique for double circuit transmission line. 2012 Fourth International Conference on Computational Intelligence and Communication Networks. pp 824–830
31. França IA, Vieira CW, Ramos DC, Sathler LH, Carrano EG (2022) A machine learning-based approach for comprehensive fault diagnosis in transmission lines. *Comput Electric Eng* 101:108107
32. Fahim SR, Sarker SK, Muyeen S, Das SK, Kamwa I (2021) A deep learning based intelligent approach in detection and classification of transmission line faults. *Int J Electr Power Energy Syst* 133:107102
33. Jiao Z, Wu R (2018) A new method to improve fault location accuracy in transmission line based on fuzzy multi-sensor data fusion. *IEEE Transact Smart Grid* 10(4):4211–4220
34. Tabari M, Sadeh J (2022) Fault location in series-compensated transmission lines using adaptive network based fuzzy inference. *Electric Power Syst Res* 208:107800

35. Ahmadipour M, Othman MM, Bo R, Salam Z, Ridha HM, Hasan K (2022) A novel microgrid fault detection and classification method using maximal overlap discrete wavelet packet transform and an augmented Lagrangian particle swarm optimization support vector machine. *Energy Rep* 8:4854–4870
36. Jimenez HA, Guillen D, Tapia-Olvera R, Escobar G, Beltran-Carbajal F (2021) An improved algorithm for fault detection and location in multi-terminal transmission lines based on wavelet correlation modes. *Electric Power Syst Res* 192:106953
37. Zhang C, Chen L, Tong Z (2022) Multi-objective optimization of heat sink with multi cross ribbed FNS for a motor controller. *J Eng Appl Sci* 69:34
38. Swelem S, Fahmy A, Ellafy H (2022) Optimization of cold formed lipped C-section under bending using prediction equations as objective functions. *J Eng Appl Sci* 69:49
39. Zhao W, Du C, Jiang S (2018) An adaptive multiscale approach for identifying multiple flaws based on XFEM and a discrete artificial fish swarm algorithm. *Comput Methods Appl Mech Eng* 339:341–357
40. Darwish A (2018) Bio-inspired computing: algorithms review, deep analysis, and the scope of applications. *Future Comput Inform J* 3(2):231–246
41. Valdez F, Castillo O, Melin P (2021) Bio-inspired algorithms and its applications for optimization in fuzzy clustering. *Algorithms* 14(4):122
42. Verma P, Parouha RP (2021) An advanced hybrid meta-heuristic algorithm for solving small-and large-scale engineering design optimization problems. *J Electric Syst Inform Technol* 8:10
43. Dommel HW (1969) Digital computer solution of electromagnetic transients in single-and multiphase networks. *IEEE Transact Power App Syst PAS* 88(4):388–399
44. Ghazizadeh Ahsae M (2012) Accurate NHIF locator utilizing two-end unsynchronized measurements. *IEEE Trans Power Del* 28(1):419–426
45. Novosel D, Phadke A, Saha MM, Lindahl S (2005) Problems and solutions for microprocessor protection of series compensated lines. *Sixth International Conference on Developments in Power System Protection*. pp 695–701
46. Sadeh J, Hadjsaid N, Ranjbar A, Feuillet R (2000) Accurate fault location algorithm for series compensated transmission lines. *IEEE Trans Power Del* 15(3):1027–1033
47. Ahmed AS, Attia MA, Hamed NM, Abdelaziz AY (2017) Modern optimization algorithms for fault location estimation in power systems. *Eng Sci Technol Int J* 20:1475–1485
48. Ghazizadeh-Ahsae M, Ghanbari N (2017) Particle swarm optimization algorithm-based fault location using asynchronous data recorded at both sides of transmission line. *Revue Roumaine des Sciences Techniques Serie Electrotechnique et Energetique* 62(2):148–153
49. Mustari MR, Hashim MN, Osman MK, Ahmad AR, Ahmad F, Ibrahim MN (2019) Fault location estimation on transmission lines using neuro-fuzzy. *Procedia Comput Sci* 163:591–602
50. Maner AS, Lavand S (2018) Accurate fault location estimation of high voltage transmission line using disturbance record. *International Conference on Power, Energy, Control and Transmission Systems (ICPECTS) 2018*. pp 26–30

Publisher's Note

Springer Nature remains neutral with regard to jurisdictional claims in published maps and institutional affiliations.